

Chapter 3

Establishing the CRISPR-Cas9 technology in primary mouse T cells

3.1 Introduction

Before the advent of CRISPR, gene expression was primarily modulated using siRNAs, which trigger degradation of mRNA (Dorsett and Tuschl, 2004). The effect of siRNAs is transient and often results in only partial protein knockdown. In contrast, CRISPR has the potential to stably and homozygously KO genes, resulting in permanent loss of gene function. While the siRNA technique was previously established in CTLs (Stinchcombe et al., 2015), the CRISPR technology was yet to be tested in primary mouse CTLs at the start of this project.

To test whether gene manipulation technologies are working as expected it is desirable to use target genes where the KO has a known CTL phenotype. Studies of patients suffering from immunodeficiency diseases have identified several suitable genetic targets. For example, mutations in *RAB27A* can cause GS2 in humans (Clark and Griffiths, 2003). This disease is the consequence of *RAB27A* deficient CTL not being able to kill target cells due to a degranulation defect. A study using CTL derived from *Rab27a* KO mice showed that while lytic granules polarise towards the immunological synapse, they cannot be secreted (Stinchcombe et al., 2001a). This indicated that *RAB27A* is involved in the final stages of granule secretion. Similarly, mutation of *MUNC13-4* causes FHL3 due to a degranulation defect (Bossi and Griffiths, 2005; Dieckmann et al., 2016; Feldmann et al., 2003). In fact, *RAB27A* and *MUNC13-4* interact with one another in this process (Neeft et al., 2005). Perforin is another protein with a well understood function in CTL cytotoxicity. Perforin defective CTL are unable to kill target cells, causing the immunodeficiency disease FHL2

(Stepp et al., 1999). These immunodeficiency diseases demonstrate the importance of correct CTL function.

3.1.1 Chapter aims

- Test the robustness of the degranulation assay and adapt it for screening.
- Manipulate gene expression in primary mouse CTLs using siRNA.
- Optimise the CRISPR-Cas9 technology in primary mouse CTLs.
- Use the CRISPR-Cas9 technology in primary mouse CTLs to target genes where the KO has a known phenotype in the degranulation assay.

3.2 Results

3.2.1 The effect of *Rab27a* depletion on CTL degranulation

CTLs derived from the *ashen* mouse model, where a mutation in *Rab27a* results in loss of protein expression, cannot kill target cells as they are unable to release their granule content (Stinchcombe et al., 2001a; Wilson et al., 2000). CTLs derived from *ashen* mice were tested in a degranulation assay, which measures lytic granule secretion by the appearance of the granule membrane component LAMP1 on the extracellular surface (Figure 3.1). The exposed extracellular LAMP1 can be bound by a fluorescently-conjugated antibody to allow robust detection and quantification of the amount of degranulation by flow cytometry. Figure 3.1A shows the gating strategy typically used in degranulation experiments. The LAMP1 gate was set so that the signal in the experimental control, which were unstimulated CTLs, was less than 1%. The percentage of degranulated (LAMP1-PE) positive cells was determined after 45 min, 90 min and 180 min. CTLs derived from homozygous (hom, *ash/ash*) *ashen* mice degranulated significantly less than CTLs derived from heterozygous (het, *+/ash*) *ashen* mice or WT (*+/+*) mice (Figure 3.1B-D) [45 min (n=2), 90 min (n=2) and 180 min (n=3, p<0.05, paired t-test)]. RAB27A protein expression in CTLs derived from WT, het and hom *ashen* mice was tested by WB, confirming that hom *ashen* CTL did not express RAB27A protein (Figure 3.1E).

Due to the robust loss of degranulation observed in *ashen* CTL, *Rab27a* provided a suitable target to test whether manipulation of gene expression in CTLs derived from WT

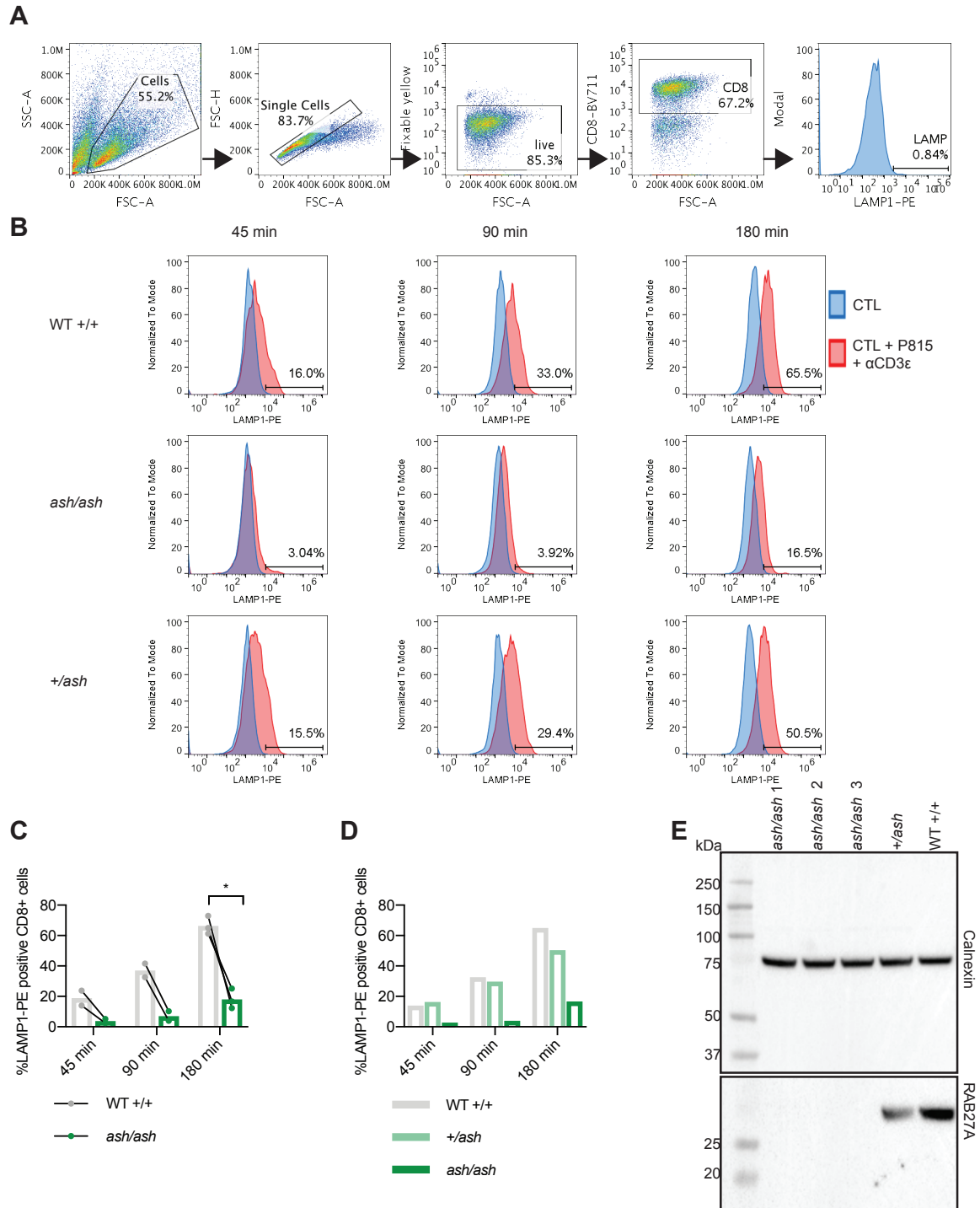


Fig. 3.1 Degranulation defect in CTL derived from *ashen* mice.

Fig. 3.1 Degranulation defect in CTL derived from ashen mice. **A** Degranulation assays were analysed using the following gating strategy: initial gate to separate the cell population from debris, second gate to isolate single cells from doublets, third gate to isolate live cells from dead cells, fourth gate to isolate CD8-positive cells and a final gate to isolate LAMP1-PE positive cells. **B** CTLs were derived from WT (+/+), het (+/ash) or hom (ash/ash) ashen mice. At day 6-7 after *in vitro* stimulation CTLs were tested for their ability to degranulate in response to exposure to α CD3 ϵ -loaded P815 target cells. Representative histograms for CTLs incubated on their own (blue histograms) or mixed at an E:T ratio of 1:1 with α CD3 ϵ -loaded P815 target cells (red histograms) for 45 min, 90 min or 180 min are shown. **C** Average degranulation result. During each independent repeat the experiment was performed at least in technical duplicates, $n=2/3$ independent experiments, * $p<0.05$ calculated by paired *t*-test. Samples were paired by day of experiment. **D** One experiment from C that included CTL from het (+/ash) ashen mice. **E** Western blot showing RAB27A and calnexin (loading control) protein expression in cells derived from WT (+/+), hom (ash/ash) and het (+/ash) ashen mice. WT = wild-type, het = heterozygous, hom = homozygous.

mice could decrease degranulation. Initially, this was attempted using a pool of siRNAs targeting Rab27a mRNA, as the siRNA technique was already established in the Griffiths lab (Stinchcombe et al., 2015). CTLs were tested for their ability to degranulate one day after nucleofection with Rab27a siRNA or scramble control siRNA. Rab27a siRNA nucleofection significantly decreased degranulation at all time points tested [45 min ($n=8$, $p<0.05$, paired *t*-test), 90 min ($n=8$, $p<0.001$, paired *t*-test) and 180 min ($n=8$, $p<0.01$, paired *t*-test)] (Figure 3.2A-B). However, the decrease was not as striking as observed with *ashen* CTL (Figure 3.1). WB showed that RAB27A protein levels were never fully depleted, but reproducibly decreased, in response to siRNA treatment (Figure 3.2C-D) ($n=7$, $p<0.01$, one sample *t*-test).

As treatment with 3 μ g siRNA did not fully deplete RAB27A protein levels after one day, protein levels were tested 2 and 3 days post nucleofection. However, longer treatment time did not reduce RAB27A protein further (Figure 3.3A). Additionally, RAB27A protein levels were not further decreased when the amount of siRNA was doubled (to 6 μ g) (Figure 3.3B). In a final attempt to improve the loss of RAB27A protein, CTLs were transfected with 3 μ g siRNA and left to recover for two days before a second transfection with 3 μ g siRNA (Figure 3.3C). However, this 'double hit' did not deplete RAB27A protein further than treatment with 3 μ g siRNA for one day (Figure 3.2D and Figure 3.3A).

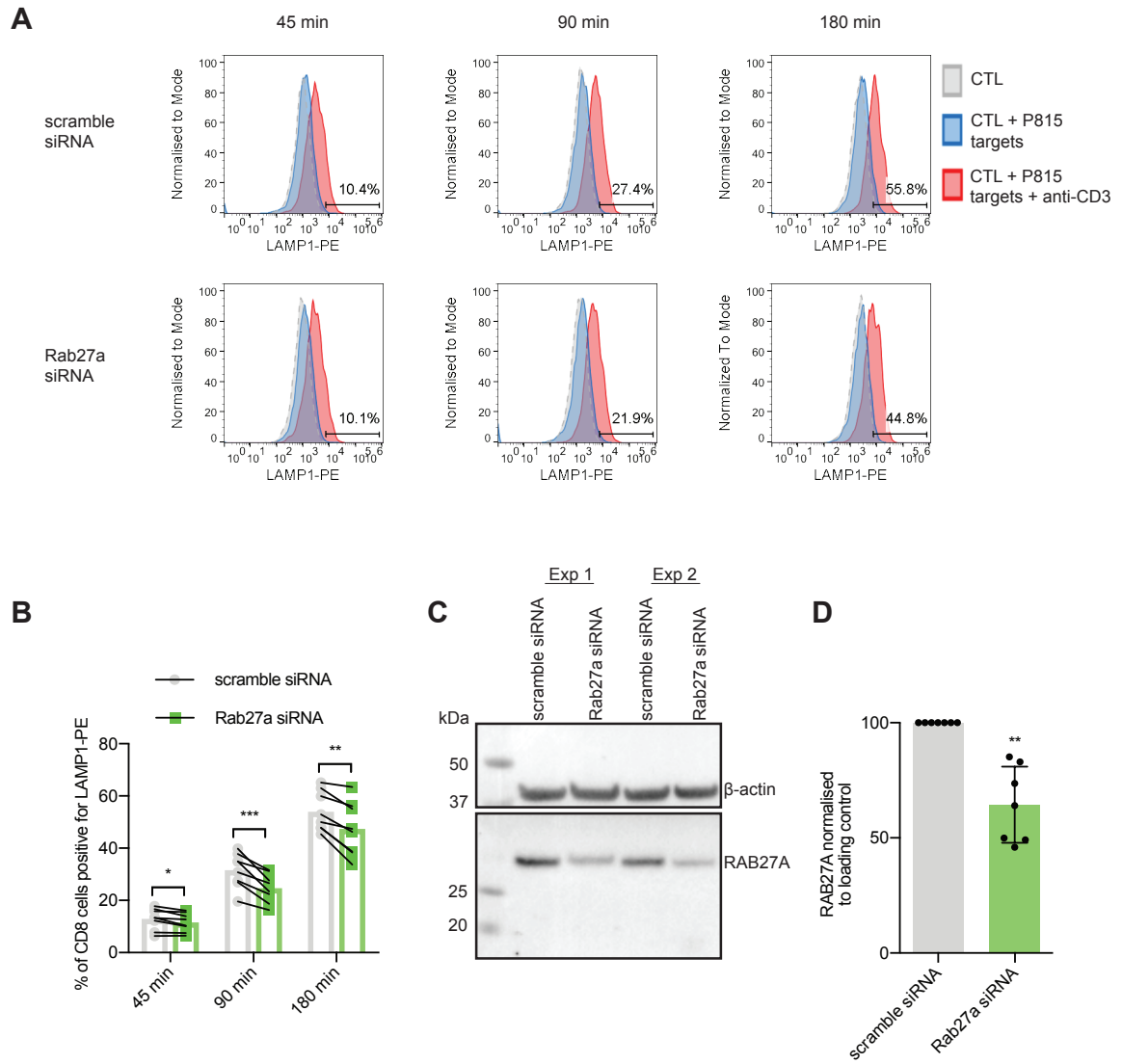


Fig. 3.2 *RAB27A* knockdown in WT mouse CTLs decreased degranulation.

Fig. 3.2 RAB27A knockdown in WT mouse CTLs decreased degranulation. **A** CTLs were nucleofected with 3 μ g scramble siRNA or 3 μ g Rab27a siRNA at day 5-7 after *in vitro* stimulation. Degranulation assays were performed the following day. Representative histograms for unstimulated CTL (grey), CTL co-cultured with P815 target cells (blue) and CTL co-cultured with α CD3 ϵ -loaded P815 target cells (red) are shown. Degranulation was measured by extracellular exposure of LAMP1 after 45 min, 90 min and 180 min. Degranulation assays were analysed using the following gating strategy: initial gate to separate the cell population from debris, second gate to isolate single cells from doublets, third gate to isolate live cells from dead cells, fourth gate to isolate CD8-positive cells and a final gate to isolate LAMP1-PE positive cells. **B** Average degranulation result, each independent experiment was performed at least in technical duplicates. $n=8$ independent experiments, $*p<0.05$, $**p<0.01$, $***p<0.001$ calculated by paired *t*-test according to the days the experiments were performed on. **C** Western blot showing RAB27A and β -actin (loading control) protein expression one day after scramble or Rab27a siRNA nucleofection in two independent experiments. **D** Average RAB27A protein knockdown achieved. In each repeat the RAB27A protein level was expressed relative to the RAB27A level in the respective scramble siRNA sample and normalised to calnexin or β -actin loading controls. Bar graphs show the mean, error bars show the SD, $n=7$ independent experiments, $**P<0.01$ calculated by one sample *t*-test. *exp* = experiment.

3.2.2 Optimising the CRISPR technology in primary mouse CTL

Rab27a was established as a good genetic target to test CRISPR, as a decrease in degranulation could be observed despite only partial protein depletion. However, for the initial set up of the CRISPR technique in CTL it would be desirable to be able to monitor KO efficiency at single cell resolution, rather than using a technique like WB, which measures a bulk population. Therefore, CRISPR was used to target the cell surface protein Thy1.2 (also known as CD90.2), referred to as Thy1 from now on. Thy1 is a glycosylphosphatidylinositol-anchored cell surface protein, which is abundantly expressed in mouse T cells (Haeryfar and Hoskin, 2004; Killeen, 1997). Due to the extracellular expression of Thy1 and the availability of good antibodies it can be easily monitored at single cell resolution using flow cytometry (Doench et al., 2014).

CTLs were derived from homozygous Cas9 mice (Tzelepis et al., 2016) and nucleofected with synthetic crRNAs and tracrRNAs. The concentration of 3 μ g used for siRNA experiments was used as a starting point for a concentration response with the CRISPR RNAs. The

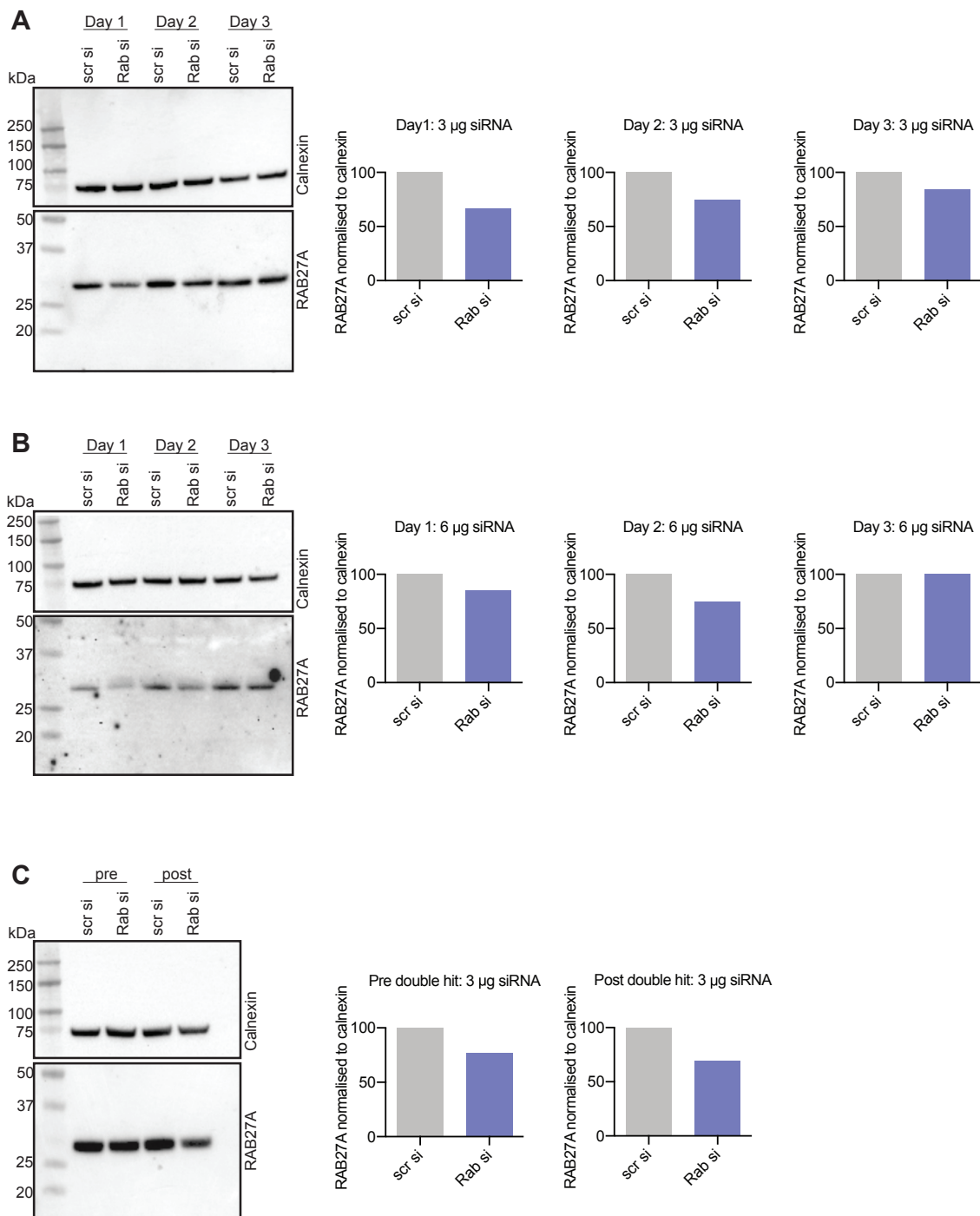


Fig. 3.3 *Optimisation of RAB27A knockdown in WT mouse CTL.*

Fig. 3.3 Optimisation of RAB27A knockdown in WT mouse CTL. **A** CTLs were nucleofected with 3 μ g scramble siRNA or 3 μ g Rab27a siRNA and RAB27A protein expression was monitored by WB over 3 days, $n=1$ for each time point. **B** CTLs were nucleofected with 6 μ g scramble siRNA or 6 μ g Rab27a siRNA and RAB27A protein expression was monitored by WB over 3 days, $n=1$ for each time point. **C** CTLs were nucleofected with 3 μ g scramble siRNA or 3 μ g Rab27a siRNA. Two days later, the same cells were nucleofected again with 3 μ g scramble siRNA or 3 μ g Rab27a siRNA. RAB27A protein expression was monitored by WB before and after the siRNA double hit, $n=1$ for each time point. In all experiments, RAB27A protein levels were normalised to calnexin (loading control) and expressed relative to the RAB27A level in the respective scramble siRNA sample. *scr si* = scramble siRNA, *Rab si* = Rab27a siRNA.

expression of Thy1 on the cell surface of CD8 T cells was monitored by flow cytometry over 5 consecutive days (Figure 3.4A). Toxicity was sometimes observed in response to nucleofecting 10 μ g crRNA reagents, as demonstrated by less events recorded in the 10 μ g *Thy1* crRNA sample in Figure 3.4A. While almost all samples were 100% positive for Thy1 at day 1 post nucleofection, by day 2 post nucleofection a decrease in the Thy1-positive population could be observed in the samples nucleofected with *Thy1* CRISPR reagents. The Thy1 levels in samples nucleofected with a non-targeting control crRNA remained unchanged. The decrease became more prominent at day 3 post nucleofection, and was stably maintained up until the final time point measured (day 5 post nucleofection). The greatest decrease in the Thy1 positive population was observed with 10 μ g crRNA/tracrRNA (average decrease of 41.6% at day 5 post nucleofection), closely followed by 5 μ g crRNA/tracrRNA (average decrease of 33.3% at day 5 post nucleofection) and then 3 μ g crRNA/tracrRNA (average decrease of 28.8% at day 5 post nucleofection) (Figure 3.4B). To avoid toxic side effects and overloading the cells with RNA, while also giving the highest chance of generating KOs, 5 μ g crRNA/tracrRNA was chosen as the amount to use in future experiments.

While KO of Thy1 using the approach outlined in Figure 3.4 worked reproducibly, it depended on the availability of Cas9 homozygous mice. While these experiments were being conducted, another study was published that used Cas9 protein alongside synthetic crRNA/tracrRNA (forming RNP complexes) in human T cells (Schumann et al., 2015). Co-nucleofection of Cas9 protein alongside crRNA and tracrRNA was tested in cells derived from OT-I mice, which were readily available in the Griffiths lab. OT-I mice express TCRs that recognise the OVA peptide in the context of H-2K^b MHC class I molecules (Hogquist

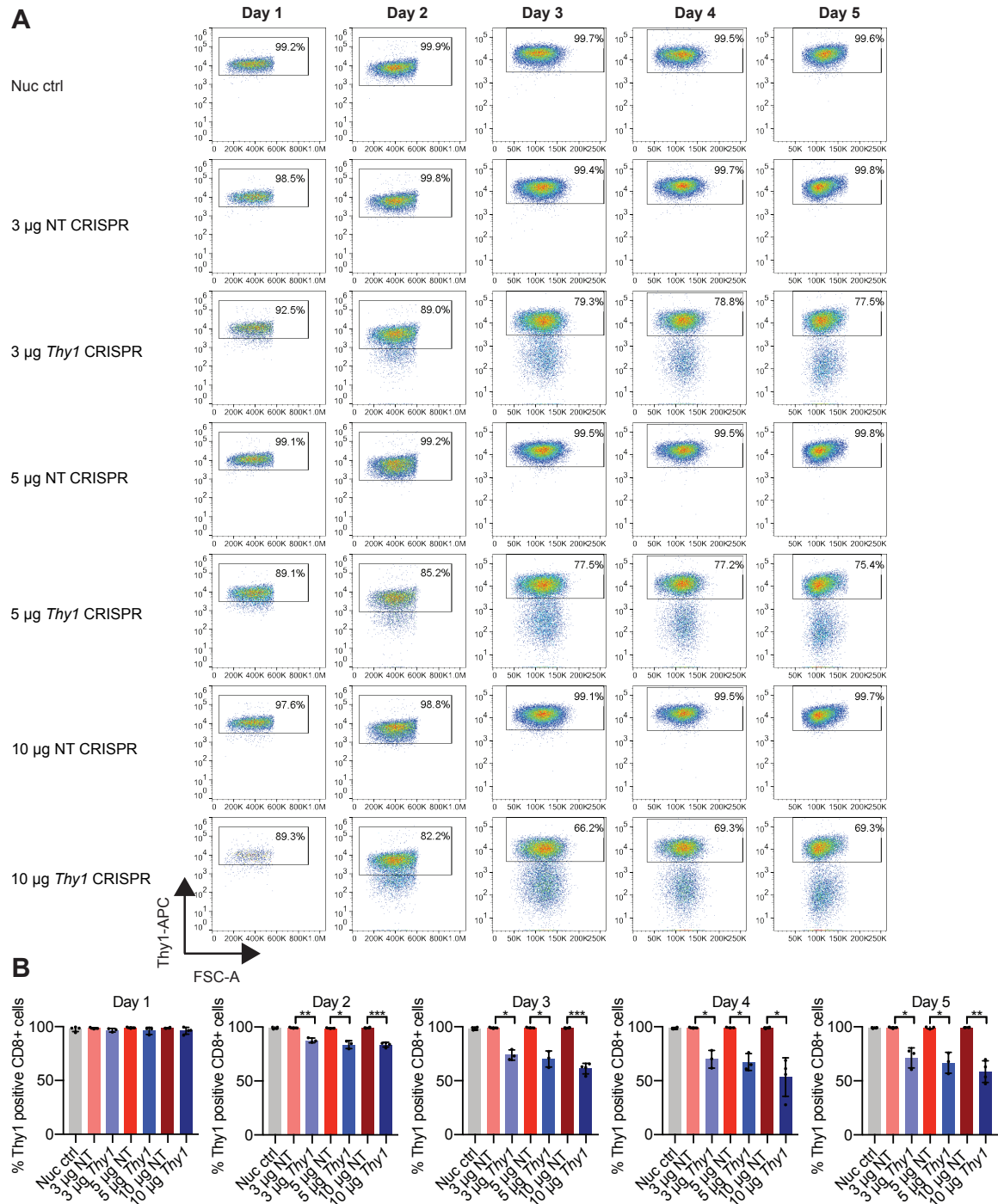


Fig. 3.4 *CrRNA* and *tracrRNA* concentration response and time course.

Fig. 3.4 *CrRNA and tracrRNA concentration response and time course.* **A** *Cas9* hom CTLs were nucleofected with the indicated amount of non-targeting or *Thy1* crRNA, in addition to the identical amount of tracrRNA at day 5-7 after *in vitro* stimulation. Additionally, a nucleofection control was included, where CTLs were nucleofected but not exposed to any RNA. *Thy1* cell surface protein levels were monitored by flow cytometry over 5 days and analysed using the following gating strategy: initial gate to separate cell population from debris, second gate to isolate single cells from doublets, third gate to isolate live cells from dead cells, fourth gate to isolate CD8-positive cells and a final gate to determine the percentage of *Thy1* positive cells. The *Thy1* gate was set according to the appropriate nucleofection control for every time point. **B** Average of *Thy1* cell surface expression in CD8 cells over the course of 5 days, $n=4$ independent experiments for nuc ctrl, 10 μg NT and 10 μg *Thy1* samples, $n=3$ independent experiments for all other samples. Bar graphs show the mean, error bars the SD, $*p<0.05$, $**p<0.01$, $***p<0.001$ calculated by unpaired *t*-test with Welch's correction. Nuc ctrl = Nucleofection control, NT = non-targeting.

et al., 1994). OT-I were nucleofected with 5 μg *Thy1* crRNA/tracrRNA and varying amounts of Cas9 protein (Figure 3.5A). As in Figure 3.4 the cell surface expression of *Thy1* was monitored by flow cytometry over 5 consecutive days. Again, a decrease in the *Thy1*-positive population could be observed in the samples nucleofected with *Thy1* CRISPR reagents, but not in cells nucleofected with non-targeting control crRNA (Figure 3.5A). This decrease was stably maintained up until the final time point (day 5 post nucleofection). The greatest decrease in the *Thy1* positive population was observed with 10 μg Cas9 (average decrease of 64.7% at day 5 post nucleofection), followed by 5 μg Cas9 (average decrease of 44.9% at day 5 post nucleofection) and then 2.5 μg Cas9 (average decrease of 29.5% at day 5 post nucleofection) (Figure 3.5B). Therefore, 10 μg Cas9 protein was chosen as the amount to use in future experiments.

To understand why *Thy1* KO was more efficient using Cas9 protein than using CTLs derived from Cas9 homozygous mice, Cas9 protein levels in samples derived from Cas9 hom mice or conditions outlined in Figure 3.5 were investigated. Cas9 levels were much higher in samples one day after nucleofection with 5 μg or 10 μg of Cas9 protein than in the samples derived from Cas9 homozygous mice (Figure 3.6A-B). Additionally, I tested whether using 20 μg Cas9 protein further increases KO efficiency, but this was not the case (Figure 3.6C). Finally, Cas9 levels were monitored over 3 days post nucleofection of Cas9 protein, demonstrating that the nucleofected Cas9 protein is only present transiently in cells,

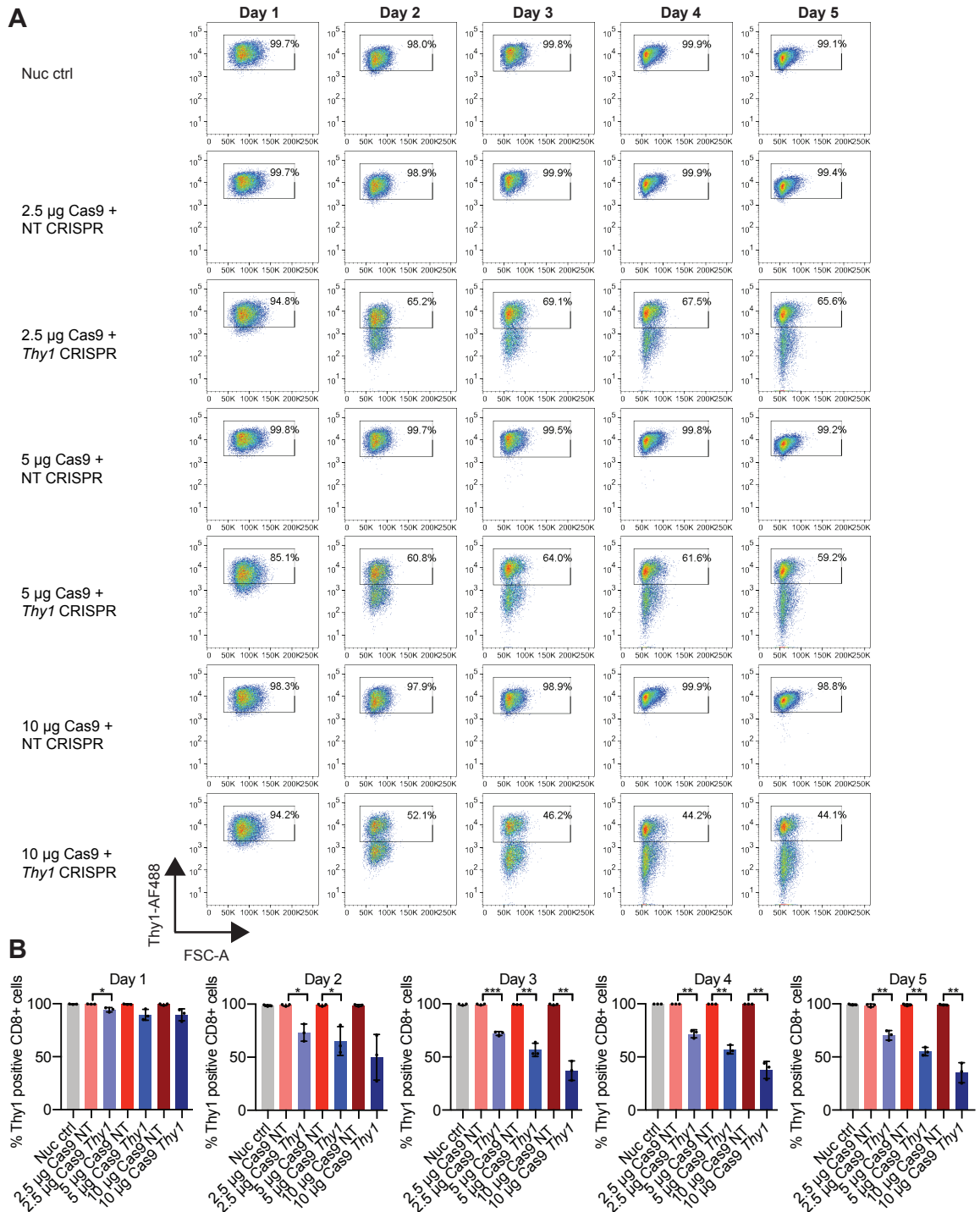


Fig. 3.5 Titration of Cas9 protein for use with synthetic crRNA and tracrRNA.

Fig. 3.5 Titration of Cas9 protein for use with synthetic crRNA and tracrRNA. **A** OT-I CTLs were nucleofected with the indicated amount of Cas9 protein in addition to 5 μ g tracrRNA and 5 μ g crRNA targeting *Thy1* or a non-targeting control crRNA at day 4 after *in vitro* stimulation. Additionally, a nucleofection control was included, where CTLs were nucleofected but not exposed to any RNA or protein. *Thy1* cell surface protein levels were monitored by flow cytometry over 5 days and analysed using the following gating strategy: initial gate to separate cell population from debris, second gate to isolate single cells from doublets, third gate to isolate live cells from dead cells, fourth gate to isolate CD8-positive cells and a final gate to determine the percentage of *Thy1* positive cells. The *Thy1* gate was set according to the appropriate nucleofection control for every time point. **B** *Thy1* cell surface expression in CD8 cells over the course of 5 days, n=3 independent experiments. Bar graphs show the mean, error bars the SD, * p <0.05, ** p <0.01, *** p <0.001 calculated by unpaired *t*-test with Welch's correction. Nuc ctrl = Nucleofection control, NT = non-targeting.

and all Cas9 protein is lost by day 2 post nucleofection (Figure 3.6D).

3.2.3 Targeting genes that are crucial for CTL killing function by CRISPR

After successfully optimising the CRISPR-Cas9 technology for mouse CTLs by targeting *Thy1*, the optimised method was used to target *Rab27a*, due to the well established effect of RAB27A loss on degranulation (Figure 3.1), as well as *perforin* and *Munc13-4*. To ensure that the technical aspects of the experiments were working, the *Thy1* crRNA was included as an efficiency control in every experiment and co-nucleofected alongside crRNAs against the genes of interest. Therefore, each experiment included the following controls: 1) a nucleofection control, 2) CTLs nucleofected with a non-targeting crRNA, tracrRNA and Cas9 protein, and 3) CTLs nucleofected with *Thy1* targeting CRISPR reagents. Each target gene was targeted with 3 crRNAs, to increase the chances of a cut, and perhaps even a large deletion, occurring. To allow time for the protein pool to be turned over, CTLs were tested in a degranulation and a killing assay four days after nucleofection. Additionally, pellets were frozen to test protein levels by WB at this time point.

Targeting *Rab27a* by CRISPR reproducibly resulted in a decrease in degranulation in comparison to controls (Figure 3.7A-B) (n=5, p <0.05, paired *t*-test). WB for the RAB27A protein confirmed that *Rab27a* CRISPR samples expressed less RAB27A protein than *Thy1* CRISPR or nucleofection controls (Figure 3.7C-D) (n=4, p <0.05, one sample *t*-test). The

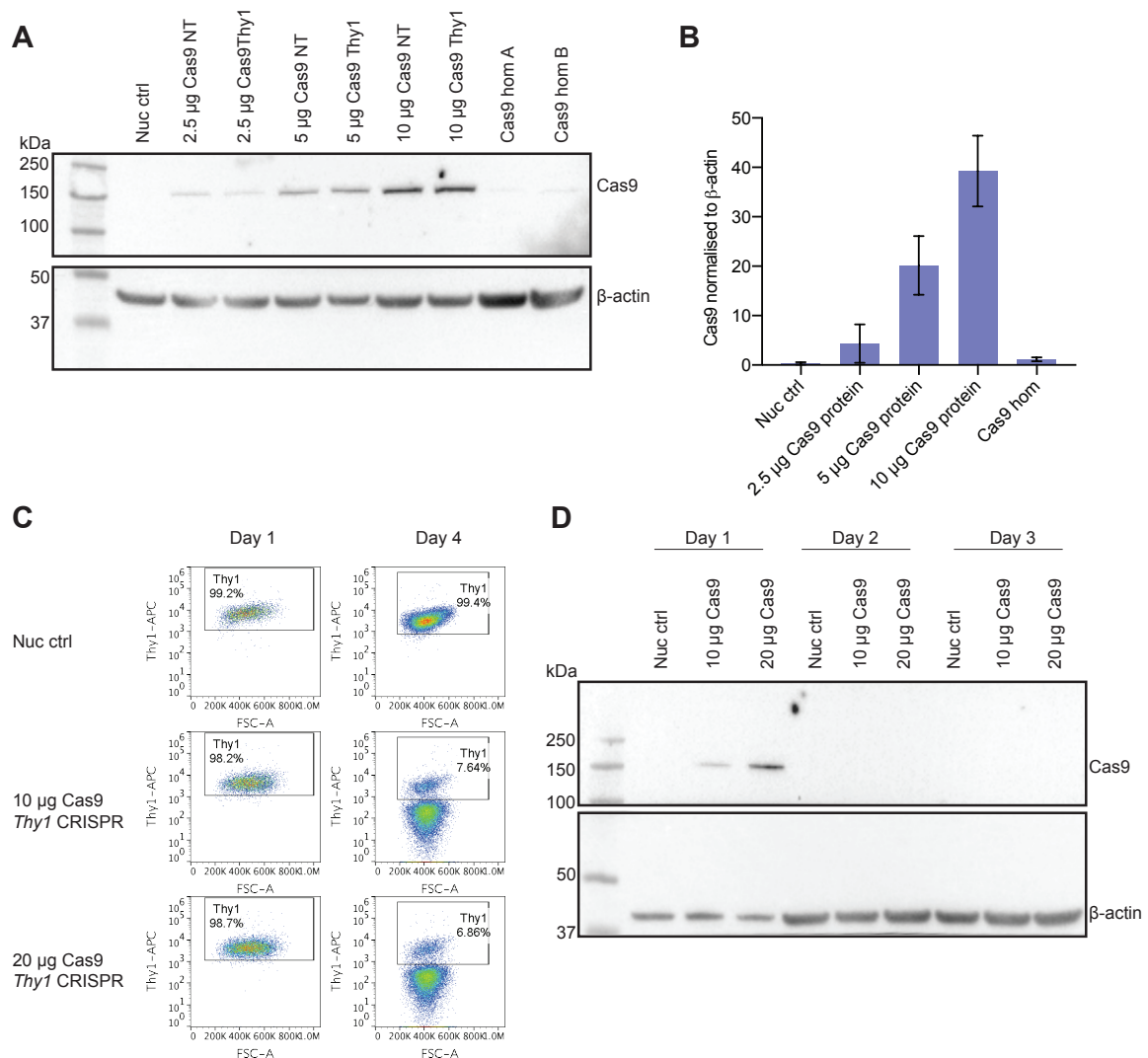


Fig. 3.6 Comparison of stable and transient Cas9 expression. **A** Representative WB showing Cas9 protein expression levels in T cells derived from homozygous Cas9 mice and T cells nucleofected with indicated amounts of Cas9 protein. **B** Quantification of WBs showing Cas9 protein expression levels. In each repeat, the Cas9 protein level was normalised to the β-actin loading control and expressed relative to the Cas9 hom samples. Bar graphs show the mean, error bars the SD, $n=2$ independent experiments. **C** Thy1 protein cell surface expression one day and four days after CTL nucleofection with the indicated reagents, $n=1$. **D** WB for Cas9 and β-actin (loading control) levels 1, 2 and 3 days after nucleofection with indicated amounts of Cas9 protein, $n=1$. Nuc ctrl = Nucleofection control, NT = non-targeting.

CTLs ability to kill target cells was determined by an assay that measures death of target cells stably expressing a red nuclear marker by loss of red fluorescence. There were more red target cells remaining in wells containing *Rab27a* CRISPR CTL than in control wells, meaning that less killing occurred in response to targeting *Rab27a* by CRISPR (Figure 3.7E-F).

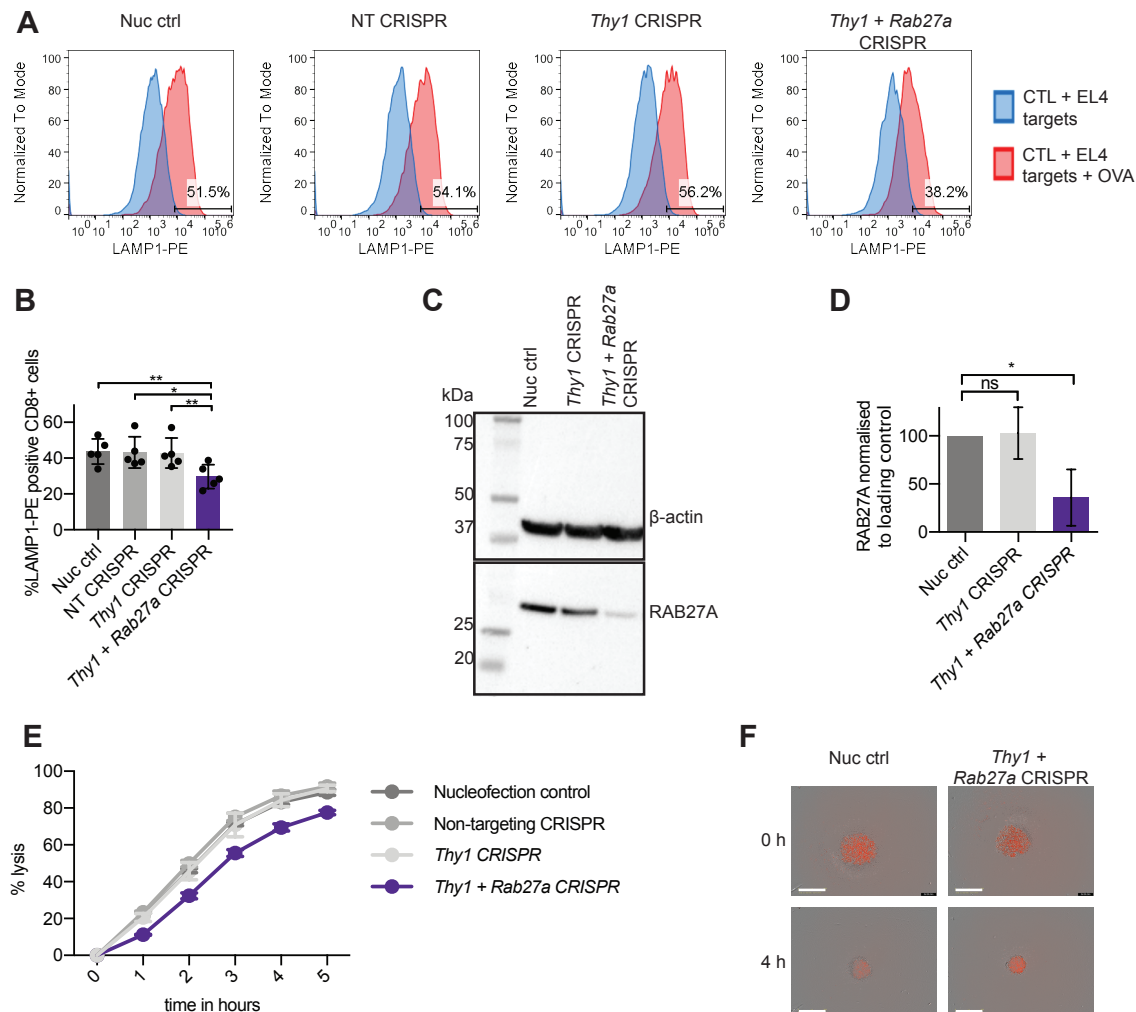


Fig. 3.7 *Decreased degranulation and killing in response to targeting Rab27a using CRISPR.*

Fig. 3.7 Decreased degranulation and killing in response to targeting Rab27a using CRISPR. OT-I CTL were nucleofected at day 4 after *in vitro* stimulation and tested in functional assays at day 8. **A** For degranulation assays CTLs were mixed with target cells at an E:T ratio of 2.5:1. Degranulation was measured by extracellular exposure of LAMP1 after 180 min. The following gating strategy was applied: initial gate to separate the cell population from debris, second gate to isolate single cells from doublets, third gate to isolate live cells from dead cells, fourth gate to isolate CD8-positive cells and a final gate to isolate LAMP1-PE positive cells. Representative histograms for unstimulated CTL co-cultured with EL4 target cells (blue) and CTL co-cultured with OVA-loaded EL4 target cells (red) are shown. **B** Average percentage of LAMP1-PE positive CD8 cells nucleofected with the indicated reagents in response to 180 min of co-culture with OVA-loaded EL4 target cells, $n=5$ independent experiments, $*p<0.05$, $**p<0.01$ calculated by paired *t*-test. Samples were paired by day of experiment. During each independent repeat the experiment was performed at least in technical duplicates. Bar graphs show the mean, error bars the SD. **C** Representative WB showing RAB27A and β -actin (loading control) protein expression four days after nucleofection. **D** Average RAB27A protein levels across 4 independent repeats. In each repeat, the RAB27A protein level was expressed relative to the nucleofection control and normalised to calnexin or β -actin loading controls. Bar graphs show the mean, error bars the SD, $*p<0.05$ calculated by one sample *t*-test, ns = not significant. **E** Incubate killing assay showing % lysis of red EL4 target cells. One representative plot for 3 independent experiments is shown. E:T = 10:1. Each datapoint is an average of 3-4 technical repeats and the error bars show the SD. **F** Raw data from Incubate killing assay showing comparable levels of red EL4 target cells between treatments at 0 h, but increased levels of red target cells in *Thy1 + Rab27a* CRISPR samples after 5 h. Scale bar = 800 μ m.

Perforin is another gene that is known to be crucial for CTL killing function. *Perforin* protein deficiency in humans causes an immunodeficiency disease (FHL2), and CTL killing is inhibited in *perforin* KO mice (Dieckmann et al., 2016; Kägi et al., 1994a; Walsh et al., 1994). However, while *perforin* KO should affect the CTLs ability to kill, it should not decrease their ability to release LAMP1 (Dieckmann et al., 2016). CTLs in which *perforin* was targeted by CRISPR did not result in a decrease in degranulation in comparison to the controls (Figure 3.8A-B). Instead, degranulation was increased in *perforin* CRISPR samples ($n=4$, $p<0.05$, paired *t*-test). Meanwhile, the CTLs ability to kill target cells was diminished, as more red target cells remained in wells containing *perforin* CRISPR CTL than in control wells (Figure 3.8E-F). Additionally, WB showed that *perforin* protein levels were decreased

in *perforin* CRISPR CTL in comparison to *Thy1* CRISPR and nucleofection control samples (n=3, P<0.001, one sample t-test) (Figure 3.8C-D).

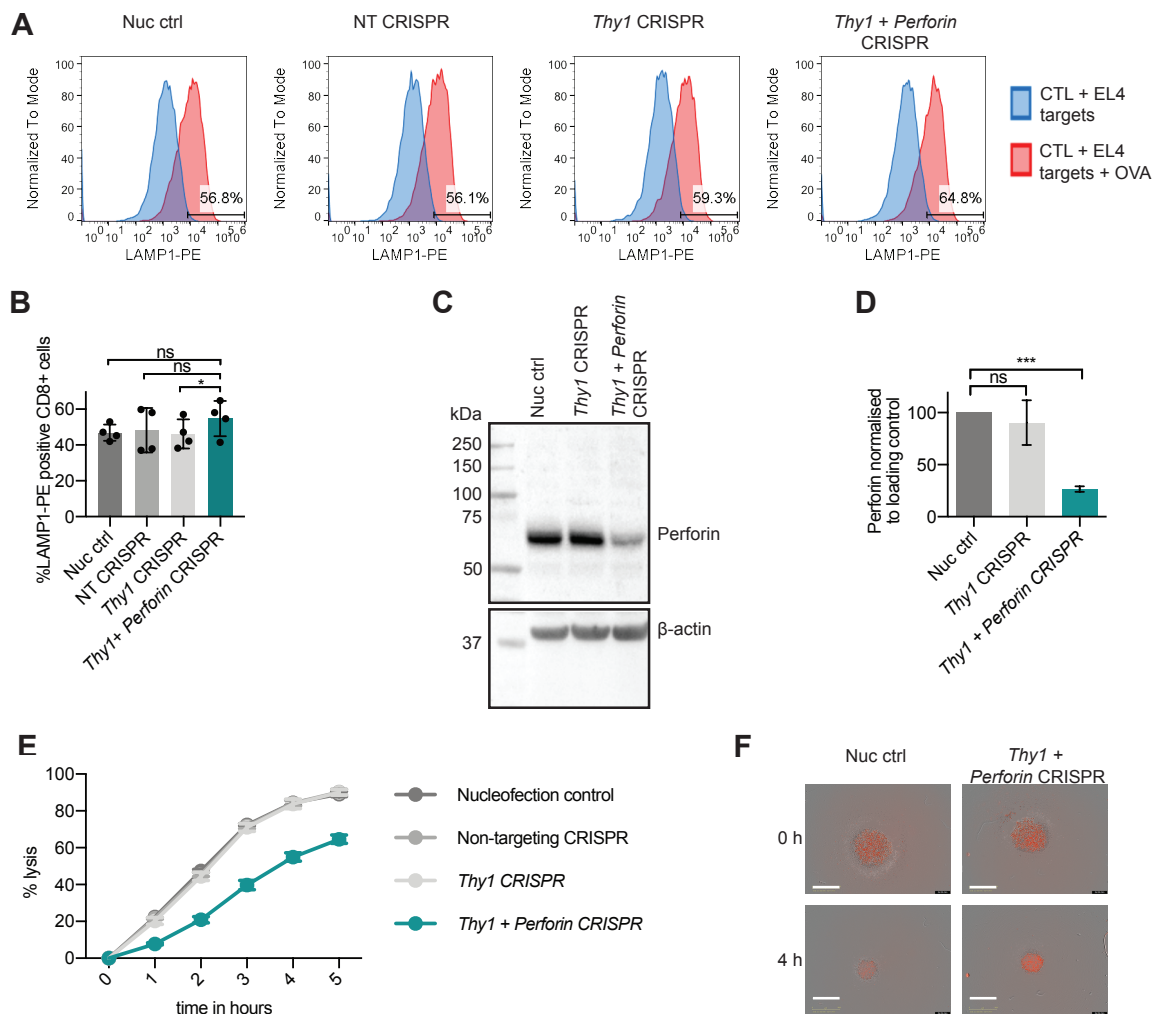


Fig. 3.8 Targeting *Perforin* by CRISPR decreased CTL killing, but not degranulation.

Fig. 3.8 Targeting Perforin by CRISPR decreased CTL killing, but not degranulation. OT-I CTL were nucleofected at day 4 after *in vitro* stimulation and tested in functional assays at day 8. **A** For degranulation assays CTLs were mixed with target cells at an E:T ratio of 2.5:1. Degranulation was measured by extracellular exposure of LAMP1 after 180 min. The following gating strategy was applied: initial gate to separate the cell population from debris, second gate to isolate single cells from doublets, third gate to isolate live cells from dead cells, fourth gate to isolate CD8-positive cells and a final gate to isolate LAMP1-PE positive cells. Representative histograms for unstimulated CTL co-cultured with EL4 target cells (blue) and CTL co-cultured with OVA-loaded EL4 target cells (red) are shown. **B** Average percentage of LAMP1-PE positive CD8 cells nucleofected with the indicated reagents in response to 180 min of co-culture with OVA-loaded EL4 target cells. Bar graphs show the mean, error bars the SD, $n=4$ independent experiments, $*p<0.05$ calculated by paired t-test, ns = not significant. Samples were paired by day of experiment. During each independent repeat the experiment was performed at least in technical duplicates. **C** Representative WB showing Perforin and β -actin (loading control) protein expression four days after nucleofection. **D** Average perforin protein levels across 3 independent repeats. In each repeat, the perforin protein level was expressed relative to the nucleofection control and normalised to calnexin or β -actin loading controls. Bar graphs show the mean, error bars the SD, $***p<0.001$ calculated by one sample t-test. **E** Incubate killing assay showing % lysis of red EL4 target cells. One representative plot for 3 independent experiments is shown. E:T = 10:1. Each datapoint is an average of 3-4 technical repeats and the error bars show the SD. **F** Raw data from Incubate killing assay showing comparable levels of red EL4 target cells between treatments at 0 h, but increased levels of red target cells in *Thy1* + Perforin CRISPR samples after 5 h. Scale bar = 800 μ m.

MUNC13-4 deficiency causes immunodeficiency in humans (FHL3) and similar phenotypes in mice (Croizat et al., 2007). Targeting *Munc13-4* by CRISPR resulted in a decrease in degranulation in comparison to controls (Figure 3.9A-B, $n=5$, $p<0.05$, paired t-test). MUNC13-4 protein levels were successfully decreased in response to CRISPR as shown by WB ($n=3$, $P<0.01$, one sample t-test) (Figure 3.9C-D). In addition to decreasing degranulation, *Munc13-4* CRISPR also decreased the ability of CTLs to kill target cells (Figure 3.9E-F).

The data generated in the *Rab27a*, *perforin* and *Munc13-4* CRISPR experiments was used to investigate whether *Thy1* expression could be used to isolate cells where the CRISPR had worked. As a crRNA against *Thy1* was co-nucleofected in these experiments, I could

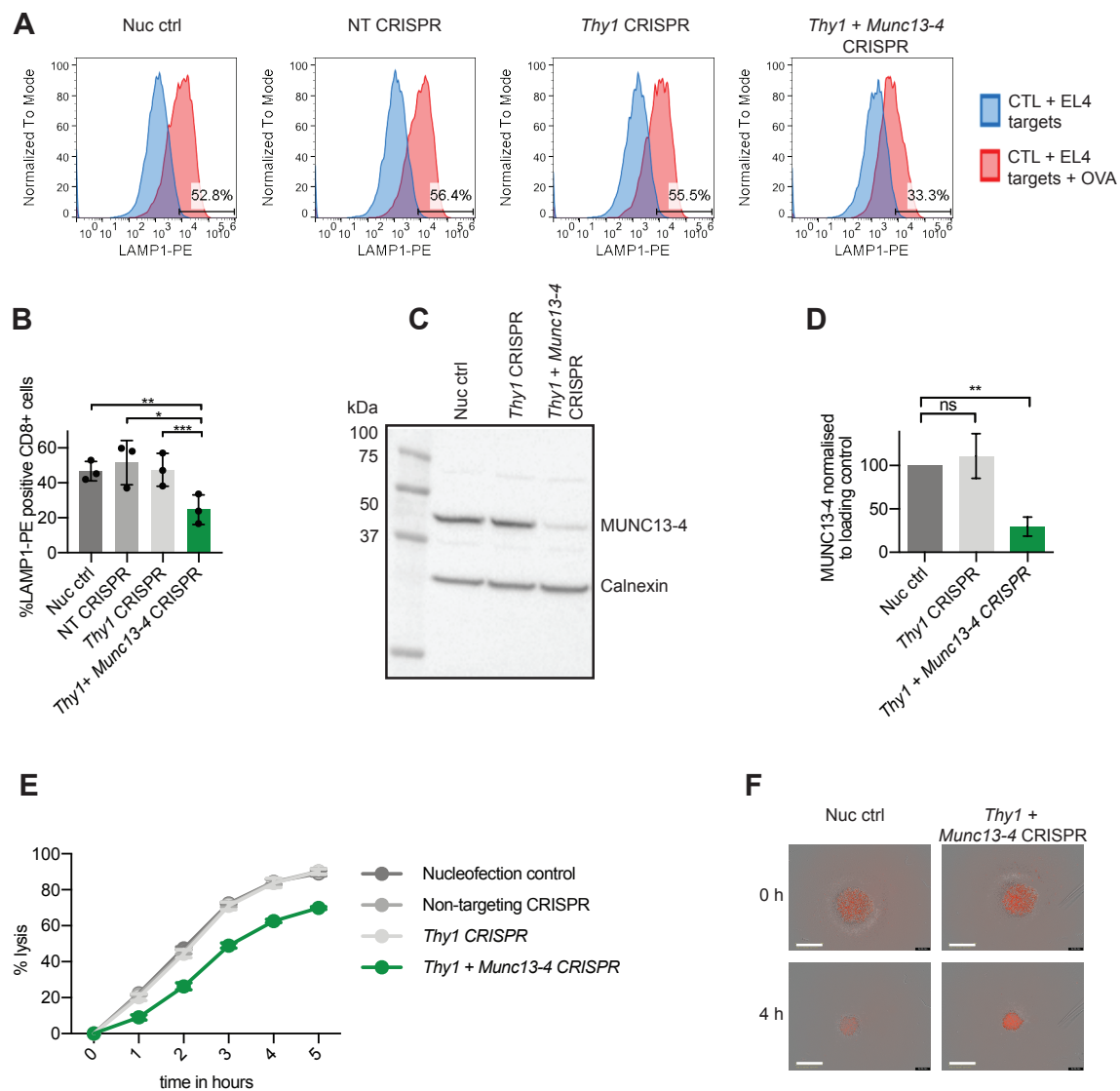


Fig. 3.9 *Munc13-4* CRISPR results in decreased degranulation and killing.

Fig. 3.9 *Munc13-4* CRISPR results in decreased degranulation and killing. OT-1 CTL were nucleofected at day 4 after *in vitro* stimulation and tested in functional assays at day 8. **A** For degranulation assays CTLs were mixed with target cells at an E:T ratio of 2.5:1. Degranulation was measured by extracellular exposure of LAMP1 after 180 min. The following gating strategy was applied: initial gate to separate the cell population from debris, second gate to isolate single cells from doublets, third gate to isolate live cells from dead cells, fourth gate to isolate CD8-positive cells and a final gate to isolate LAMP1-PE positive cells. Representative histograms for unstimulated CTL co-cultured with EL4 target cells (blue) and CTL co-cultured with OVA-loaded EL4 target cells (red) are shown. **B** Average percentage of LAMP1-PE positive CD8 cells nucleofected with the indicated reagents in response to 180 min of co-culture with OVA-loaded EL4 target cells. Bar graphs show the mean, error bars the SD, $n=3$ independent experiments. During each independent repeat the experiment was performed at least in technical duplicates. **C** Representative WB showing MUNC13-4 and calnexin (loading control) protein expression four days after nucleofection. **D** Average MUNC13-4 protein levels across 3 independent repeats. In each repeat, the MUNC13-4 protein level was expressed relative to the nucleofection control and normalised to calnexin loading controls. Bar graphs show the mean, error bars the SD, $***p<0.01$ calculated by one sample *t*-test, *ns* = not significant. **E** Incucyte killing assay showing % lysis of red EL4 target cells. One representative plot for 3 independent experiments is shown. E:T = 10:1. Each datapoint is an average of 3-4 technical repeats and the error bars show the SD. **F** Raw data from Incucyte killing assay showing comparable levels of red EL4 target cells between treatments at 0 h, but increased levels of red target cells in *Thy1 + Munc13-4* CRISPR samples after 5 h. Scale bar = 800 μm .

gate on *Thy1* negative cells during the degranulation assay. This allowed to select cells that 1) have been nucleofected successfully and 2) have taken up Cas9-RNP complexes. Data from these assays was analysed using two different gating strategies, outlined in Figure 3.10A, in order to investigate whether gating on the *Thy1*-negative population resulted in a more striking degranulation phenotype in CRISPR samples. Gating on *Thy1* negative cells showed a trend towards further decreasing the percentage of LAMP1-PE positive cells observed in *Munc13-4* and *Rab27a* CRISPR experiments, in comparison to the results obtained without gating on *Thy1* negative cells. This indicated that gating on *Thy1* negative cells could be used to isolate edited cells to some extent, however this effect was not statistically significant when tested using a paired *t*-test (Figure 3.10B).

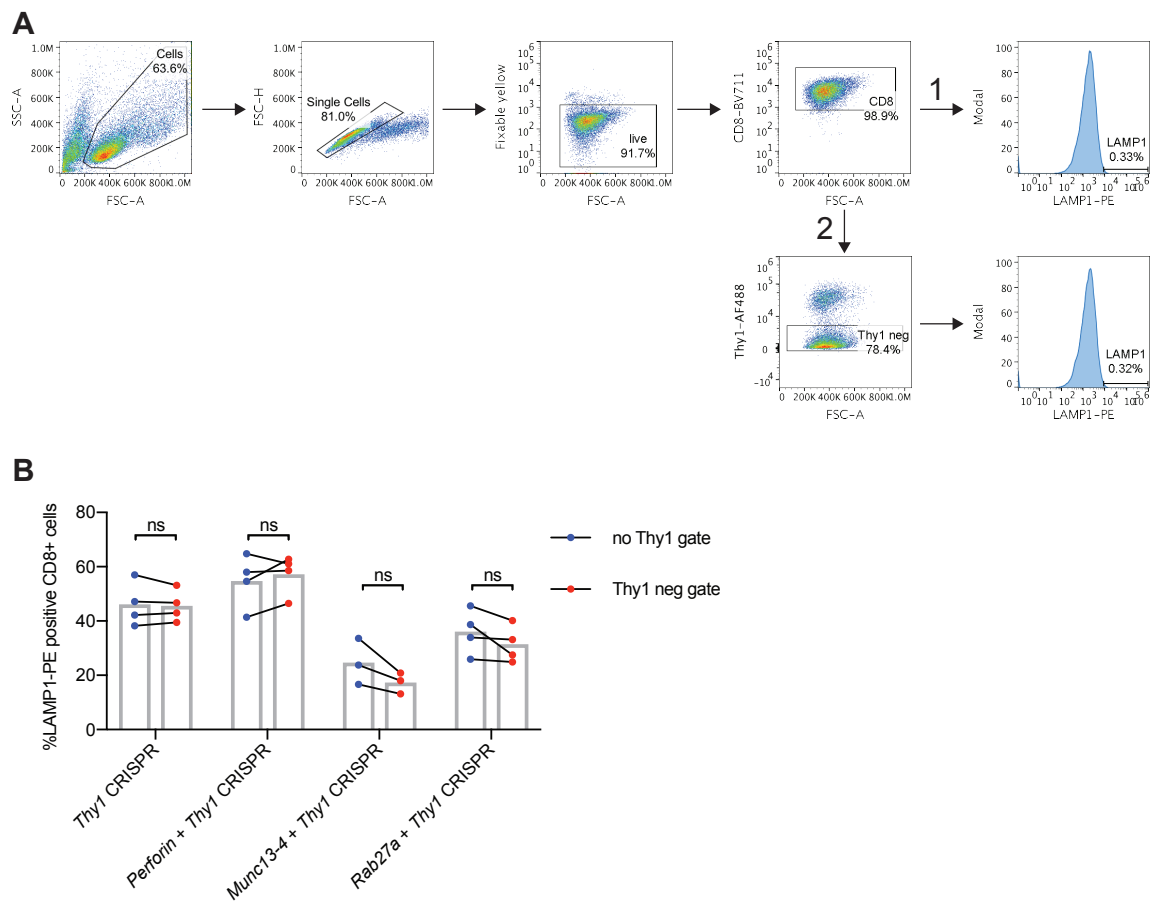
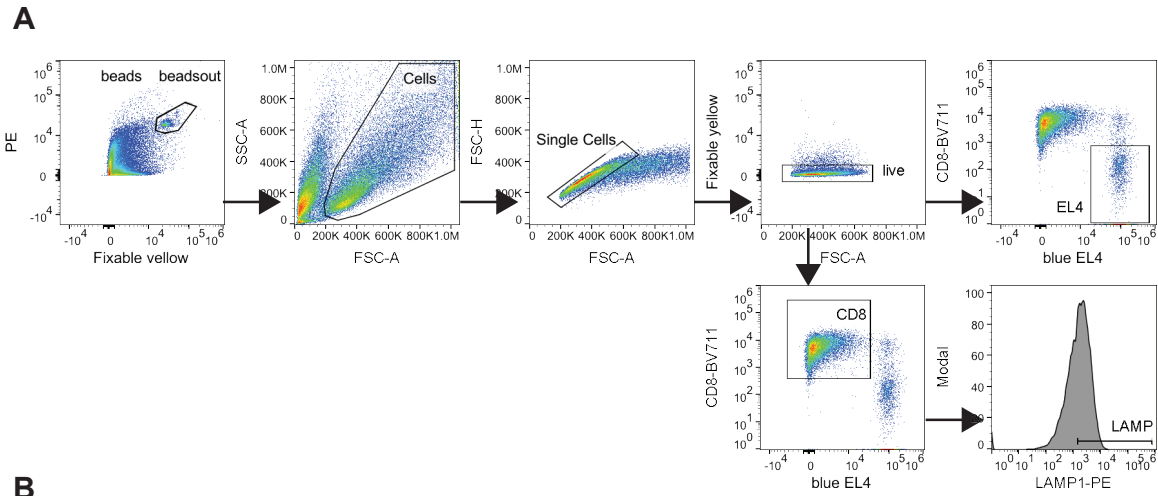


Fig. 3.10 The effect of gating on Thy1 negative cells on degranulation. **A** Degranulation assays were analysed using two gating strategies: initial gate to separate the cell population from debris, second gate to isolate single cells from doublets, third gate to isolate live cells from dead cells and a fourth gate to isolate CD8-positive cells. This was followed by either 1) a final gate to isolate LAMP1-PE positive cells or 2) a fifth gate to isolate Thy1 negative cells prior to a sixth gate to isolate LAMP1-PE positive cells. **B** Average percentage of LAMP1-PE positive CD8 cells in response to 180 min of co-culture with OVA-loaded EL4 target cells. Each experiment was analysed with gating strategy 1 (blue) and gating strategy 2 (red). The results from both gating strategies were compared using paired *t*-tests, with sample pairing by day of experiment, $n=3/4$ independent experiments. During each independent repeat the experiment was performed at least in technical duplicates. *neg* = negative, *ns* = not significant.

While a degranulation defect often overlaps with a killing phenotype, as observed for *Rab27a* and *Munc13-4* CRISPR samples (Figure 3.7 and 3.9), the *perforin* CRISPR result highlighted that some genes implicated in CTL killing could be missed if the degranulation assay is used as the sole readout in a screen. For example, genes that affect the cytolytic components of the granules, rather than granule release, could not be detected using the traditional degranulation assay. Since the aim of this project is to identify genes involved in CTL killing, an assay that measures killing as well as degranulation would be desirable. To achieve this, the standard degranulation assay was modified. Firstly, target cells stably expressing BFP (see chapter 2, section 2.1.4) were used. Secondly, a known amount of fluorescent cell counting beads was added to each sample just before analysis on the flow cytometer. Gating on these populations allowed me to determine the number of beads and the number of blue target cells that were recorded in each sample. This enabled the ratiometric enumeration of target cells, accounting for any differences in acquisition between samples. As a result, the percentage of live and dead EL4 target cells in each well could be determined at the same time as CTL degranulation was measured (Figure 3.11A,B, please see figure legend for a more detailed description of this calculation).

To test this assay, I used the *Rab27a*, *Munc13-4* and *perforin* CRISPR samples previously shown to result in protein loss and a reduced killing phenotype (Figures 3.7, 3.8, 3.9). For nucleofection control samples, the reduction of EL4 target cells can even be seen by eye when comparing the EL4 population between CTL+EL4-OVA and CTL+EL4+OVA conditions, indicating that target cell killing is occurring (Figure 3.11C). In contrast, such a decrease in the EL4 population cannot be observed for *Thy1 + Rab27a* CRISPR samples, indicating that target cell killing is reduced (Figure 3.11C). The bead method enabled quantification of this difference and allowed me to plot the percentage of target cells killed (Figure 3.11D). A decrease in target cell killing was observed for *Thy1 + Rab27a* CRISPR samples (n=3, p<0.05, paired t-test), *Thy1 + Munc13-4* CRISPR samples (n=3, p<0.05, paired t-test) and *Thy1 + perforin* CRISPR samples (n=2).



B

Sample	Count in EL4 gate	Count in beads gate	EL4:beads ratio	*10100 = no. of live EL4	% live	% dead
CTL + EL4 -OVA	2132	2540	0.84	8484		
CTL + EL4 + OVA	1276	2744	0.47	4747	55.40	44.60

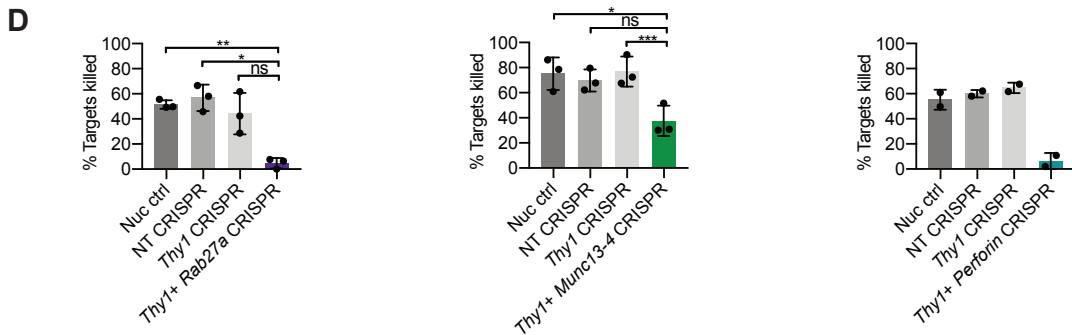
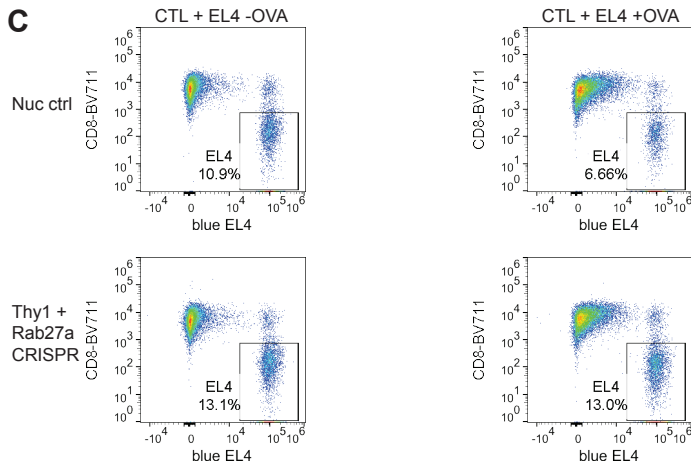


Fig. 3.11 The combined degranulation and killing assay.

Fig. 3.11 The combined degranulation and killing assay. **A** Gating strategy used to analyse the combined degranulation and killing assay. The fluorescent 123count ebeads can be separated from cells by size and using different fluorescence channels. One gate is drawn around the beads ('beads') to determine the number of beads present in the sample. Another identical gate is used to select all events except for the beads ('beadsout'), so that the beads do not interfere with any other fluorescent signal. Within the 'beadsout' gate, a gate to separate the cell population from debris is followed by a gate to isolate single cells from doublets. Next, live cells are isolated from dead cells before gating on CD8 cells to determine the degranulation readout or blue EL4 target cells to determine the target cell count. **B** Example quantification of the killing response using the beads method. The count in the EL4 gate is divided by the count in the beads gate, giving an EL4:beads ratio. This can be multiplied by the number of beads added per well (in this example 10,100 beads, information supplied by the manufacturer for every batch) to calculate the absolute number of live target cells in the well. Normalising the +OVA sample to its respective -OVA sample allows determination of the percentage of live target cells remaining in the +OVA sample. This, in turn, allowed me to deduce the percentage of dead target cells that have been killed by CTLs. **C** Representative example of the killing response of CTLs derived from nucleofection control and *Thy1 + Rab27a* CRISPR samples. In the nucleofection control sample, a decrease in blue EL4 target cells from -OVA to +OVA plots can be seen. No decrease in blue EL4 target cells could be detected between -OVA and +OVA plots from *Thy1 + Rab27a* CRISPR samples. **D** Average killing assay readout for *Thy1 + Rab27a* CRISPR ($n=3$ independent experiments), *Thy1 + Munc13-4* CRISPR ($n=3$ independent experiments) and *Thy1 + Perforin* CRISPR ($n=2$ independent experiments). E:T ratio = 2.5:1, assay duration = 180 min. Bar graphs show the mean, error bars the SD. Statistical analysis was not performed on *Thy1 + Perforin* CRISPR experiments as data was derived from only two independent experiments (see section 2.14). ns = not significant, $*p<0.05$, $**p<0.01$, $***p<0.001$ as calculated by paired *t*-test. Samples were paired by day of experiment to account for day-to-day variations.

3.3 Discussion

Figure 3.1 shows that RAB27A was expressed in CTLs derived from WT and het *ashen* mice, but not in hom *ashen* mice. CTLs derived from hom *ashen* mice furthermore showed a striking degranulation defect (Figure 3.1). Using siRNA to knockdown RAB27A protein in CTLs derived from WT mice resulted in a consistent decrease in degranulation in comparison to the respective controls. It was not possible to reproduce the striking decrease in degranulation

observed in CTLs derived from hom *ashen* mice with siRNA knockdown (Figure 3.2). The mild siRNA phenotype can be explained by only partial protein knockdown being achieved (Figure 3.2). The biggest decrease in protein level was achieved with 3 μg siRNA one day after nucleofection, but this only reduced protein levels by 36% on average (n=7). Increasing Rab27a siRNA concentration, incubation time or nucleofecting CTLs twice with siRNA did not decrease RAB27A protein levels further (Figure 3.3). This indicated either low nucleofection efficiency, or that the siRNA did not work as effectively as expected. Nonetheless, it is important to note, that even only partial RAB27A protein knockdown still reproducibly resulted in a decrease in degranulation, making *Rab27a* a good target for testing phenotypic effects of CRISPR KO.

The partial protein knockdown observed in response to Rab27a siRNA treatment highlighted the disadvantage of using a technique like WB for the detection of protein loss, as WB shows the bulk cell population. Only a small proportion of the cell population may take up the CRISPR reagents upon nucleofection. Furthermore, even in cells where CRISPR will introduce cuts in the desired gene, there will be a mixed population of heterozygous and homozygous KOs. A technique that gives single cell resolution, such as flow cytometry, allows observation of the effect even if the KO only occurs in a small subset of the entire cell population.

For ease of detection by flow cytometry, the cell surface protein Thy1 was targeted using synthetic CRISPR reagents for the initial set up of the CRISPR technique. The best KO efficiency without toxic side effects was observed with 5 μg crRNA/tracrRNA and 10 μg Cas9 protein (Figure 3.4 and 3.5). This reproducibly achieved loss of Thy1 surface expression in over 60% of the cell population (Figure 3.5B), sometimes achieving over 90% KO (Figure 3.6C). Increasing the amount of Cas9 protein beyond 10 μg did not further improve KO efficiency (Figure 3.6C). Nucleofecting Cas9 protein likely resulted in a higher KO efficiency than using CTLs from Cas9 hom mice due to the higher Cas9 level in the former samples (Figure 3.6A-B).

Time course experiments (Figures 3.4 and 3.5) showed that it took 2-3 days for the CRISPR effect to show, which indicated that this is the amount of time it took for the CRISPR-induced damage to accumulate and for the Thy1 protein pool to be turned over. As protein longevity varies greatly, it would be best to wait as long as possible to allow protein turnover when targeting other genes using CRISPR. However, mouse CTL lifespan in tissue culture is limited, and they are best used for functional assays around day 7-8 post in vitro

stimulation. Therefore, CTLs were nucleofected at day 4 post in vitro stimulation and tested in functional assays at day 8. This optimised CRISPR approach was successfully used to knock out genes that are known to be crucial for CTL killing function. Targeting *Rab27a* and *Munc13-4* decreased the degranulation and killing capabilities of CTLs (Figures 3.7 and 3.9). Targeting *perforin* affected CTL killing without decreasing degranulation (Figure 3.8).

A downside to any approach involving nucleofection of synthetic RNAs is that there is no way to select cells that have taken up the reagents. Therefore, the population studied will always be a mix of WT and genetically modified cells meaning that genes that have subtle effects upon KO may be overlooked. Because of this it is important to optimise the reagent concentration in order to maximise the KO efficiency as done in Figure 3.4 to 3.5.

To isolate cells that have been nucleofected successfully in a degranulation assay, others have co-nucleofected a GFP-plasmid alongside siRNAs (Kabanova et al., 2016). The underlying assumption is that cells which have taken up the GFP plasmid are also more likely to have taken up the co-nucleofected reagents. A more accurate approach would be to use synthetic crRNAs or tracrRNAs fused to a fluorescent marker, as done by Seki and Rutz (2018). However this fusion may affect the function of the RNA and such products were not yet available when the experiments outlined in this chapter were performed.

As an alternative approach, a *Thy1* crRNA was co-nucleofected alongside the crRNAs against the gene of interest. The percentage of Thy1 KO could be measured alongside the percentage of LAMP1-PE positive cells in the degranulation assay. In addition to allowing to monitor the nucleofection efficiency, targeting *Thy1* gave an idea of how well the CRISPR worked in each experimental condition. A lack of *Thy1* KO would indicate a technical mistake, such as accidentally not adding Cas9 protein. Using the *Thy1* readout to select cells where the CRISPR technique worked, by gating on *Thy1* negative cells in the degranulation assay, did not significantly improve the readout in *Rab27a*, *Munc13-4* or *perforin* CRISPR experiments (Figure 3.10).

While it was beneficial to co-nucleofect a *Thy1* crRNA in initial experiments to ensure the CRISPR technique was working robustly, it also raised some concerns. Firstly, targeting an additional region in the genome could result in unanticipated side effects. Secondly, it could decrease CRISPR efficiency for the gene of interest by competing for the available Cas9 and tracrRNA reagents. Thirdly, gating on *Thy1* negative cells during the degranulation assay means that I cannot meaningfully compare the data to the controls that are closest to the

unmanipulated cells (nucleofection controls and non-targeting CRISPR controls), as these do not contain a Thy1 negative population. Finally, others have suggested that Thy1 can affect T cell activation, which could result in unwanted side effects (Haeryfar and Hoskin, 2004; Killeen, 1997). In summary, I therefore concluded that it would be preferable not to co-nucleofect the *Thy1* crRNA alongside crRNAs against other genes from now on.

3.3.1 Development of an assay to measure both degranulation and killing

The degranulation assay is suitable for high throughput screening as it can be performed in a 96 well format. Picking one time point would maximise the number of samples fitting on one plate. The 90 min and 180 min time points showed the clearest separation between scramble and Rab27a siRNA treated samples (Figure 3.2). As the 180 min time point also showed a clear separation in Incucyte killing assays (Figure 3.7 to 3.9) it was chosen as the most suitable end point for the degranulation assay in an effort to miniaturise the assay.

The beads assay (Figure 3.11) allowed to determine the percentage of target cells killed in the same well as the degranulation readout. This was achieved by making two simple changes to the traditional degranulation assay: 1) the addition of stained target cells and 2) the addition of a known amount of cell counting beads. This assay will enable to test killing phenotypes at the same scale as the degranulation assay. To maximise the number of samples fitting on one plate this assay was limited to one E:T ratio and one time point. Therefore, any promising hits should be followed up further with additional phenotypic assays.

3.3.2 Summary and evaluation of aims

- Degranulation assay set up and adaptation for a screen.
 - The degranulation assay successfully showed a defect in response to RAB27A and MUNC13-4 depletion. As the 180 min time point showed a clear separation between experimental samples and controls it was chosen as the only time point to be used subsequently in order to maximise the number of samples per degranulation assay. Furthermore, an assay that simultaneously measures degranulation and killing was developed.
- Manipulate gene expression in primary mouse CTLs using siRNA.

-
- RAB27A protein levels were successfully reduced in response to treatment with Rab27a siRNA, although not to the desired extent. This highlighted the potential of CRISPR which can stably and homozygously KO genes.
 - Optimise the CRISPR-Cas9 technology in primary mouse CTLs.
 - The use of synthetic crRNA and tracrRNA reagents as well as Cas9 protein was optimised through concentration response and time course experiments targeting the cell surface protein Thy1. Conditions that resulted in reproducible and efficient KO were successfully established.
 - Use the CRISPR-Cas9 technology in primary mouse CTLs to target genes where the KO has a known phenotype in the degranulation assay.
 - *Rab27a*, *perforin* and *Munc13-4* were successfully targeted by CRISPR in mCTL as demonstrated by WB, degranulation and killing assays.

